

Design of nonuniformly spaced phase-stepped algorithms using their frequency transfer function

MANUEL SERVIN,^{*} MOISES PADILLA, GUILLERMO GARNICA, AND GONZALO PAEZ

Centro de Investigaciones en Optica A. C., Loma del Bosque 115, Col. Lomas del Campestre, Leon Guanajuato, Mexico, C. P. 37150.

*Corresponding author: mservin@cio.mx

Here we show how to design phase-shifting algorithms (PSAs) for nonuniform phase-shifted fringe patterns using their frequency transfer function (FTF). Assuming that the nonuniform/nonlinear (NL) phase-steps are known, we introduce the desired zeroes in the FTF to obtain the specific NL-PSA formula. The advantage of designing NL-PSAs based on their FTF is that one can reject many distorting harmonics of the fringes. We can also estimate the signal-to-noise ratio (SNR) for interferograms corrupted by additive white Gaussian noise (AWGN). Finally, for non-distorted noiseless fringes, the proposed NL-PSA retrieves the modulating phase error-free, just as standard/linear PSAs do.

Since the seminal work of Greivenkamp, "Generalized data reduction for heterodyne interferometry," in 1984 (G-PSA) [1], there has been an increasing interest for nonlinear phase-step PSAs (NL-PSAs) [2-10]. That is because (except for fringe projection profilometry) one cannot always guarantee pure-linear phase-shifted fringe-data [11]. Nowadays the best known NL-PSAs are: a) the generalized PSA (G-PSA) [1]; b) the advanced iterative algorithm (AIA) [2-5]; c) NL-PSAs which consider small phase-shift nonlinearity, approximated by a Taylor series [6-8], and d) the principal component analysis (PCA) of phase-shifted fringes [9,10]. The PCA-based PSA (PCA-PSA) normally requires many phase-shifted interferograms having at least one spatial fringe to obtain the estimated phase with small, non-zero error, even for noiseless fringes [9,10]. The PCA and the AIA were combined to obtain a faster AIA providing as initial condition the small-error estimation of the PCA-PSA [10]. Also we know that G-PSA, AIA, and PCA-PSA do not reject high-order harmonics of the fringes by design [1-10]. Moreover the G-PSA, AIA, and PCA-PSA do not give any estimation of the SNR of the demodulated signal [1-10]. People working on variations of G-PSA, AIA, and PCA-PSA can only make noise/harmonics robustness comparisons from specific simulated or experimental fringes [1-10]. In other words, using the available NL-PSA theory [1-10], one cannot know the SNR from basic stochastic process theory [12].

Our contribution. Here we present explicitly N -step NL-PSA formulas with a desired FTF spectral response. The NL-PSA's FTF reject the highest number of fringe harmonics for a given number of phase steps. For noiseless, non-distorted data, our NL-PSA formulas give the exact modulating phase, not just a good approximation (as other NL-PSAs do [6-10]). In simple terms, the phase recovered with our NL-PSA equals the error-free phase obtained by standard/linear PSAs for noiseless fringes [11]. Moreover, using the designed FTF, one can easily estimate the SNR from basic stochastic process theory [11,12]. This contrasts with G-PSA, AIA, and PCA-PSA which do not give any SNR figure-of-merit [1-10]. For amplitude-distorted fringes, our NL-PSA give much better results than G-PSA, AIA, or PCA-PSA because our NL-PSA explicitly rejects many harmonics. The only constrain to our FTF-based NL-PSA design is that one needs a previous estimate of the nonlinear phase-steps. But this is not difficult for spatial linear-carrier fringes, for which the Fourier method can be used, or by the use of the Carré nonlinear phase-step formula for temporal fringes with no spatial carrier [11].

Linear phase-step PSAs. Before going to the main contribution of this work, we briefly review the concept of the FTF for spectral analysis of linear phase-step PSAs. Let us start by the standard mathematical form for continuous phase-shifted fringes,

$$I(t; \varphi_{x,y}) = a_{x,y} + b_{x,y} \cos(\varphi_{x,y} + \omega_0 t). \quad (1)$$

The measuring phase is $\varphi_{x,y}$; the background of the fringes is $a_{x,y}$; the contrast is $b_{x,y}$, and the angular frequency is ω_0 . For notation economy, we will use (φ, a, b) instead of $(\varphi_{x,y}, a_{x,y}, b_{x,y})$. If our interferograms have amplitude distortion, then one must include the fringe harmonics as,

$$I(t; \varphi) = a + \sum_{k=1}^{\infty} b_k \cos[k(\varphi + \omega_0 t)]. \quad (2)$$

It is usual to express the n th sample $I(n; \varphi)$ as,

$$I(n; \varphi) = \int_{-\infty}^{\infty} I(t; \varphi) \delta(t - n) dt; \quad n \in \{0, 1, \dots, N-1\}. \quad (3)$$

Being $\delta(t-n)$ the sampling Dirac delta function. Then a linear phase-stepped PSA may be written as,

$$Ae^{i\hat{\phi}} = \sum_{n=0}^{N-1} c_n^* I(n; \varphi); \quad (c_n \in \mathbb{C}); i = \sqrt{-1}. \quad (4)$$

The asterisk denotes the complex conjugated. This system has the following impulse response,

$$h(t) = \sum_{n=0}^{N-1} c_n \delta(t-n). \quad (5)$$

Taking the Fourier transform of $h(t)$ one obtains the spectral response of the PSA (the FTF) as,

$$H(\omega) = F\{h(t)\} = \sum_{n=0}^{N-1} c_n e^{-in\omega}. \quad (6)$$

If the fringe data is corrupted by AWGN, the SNR-gain (G_{SNR}) for a linear N -step PSAs is given by [11],

$$G_{\text{SNR}} = \frac{\left| \sum_{n=0}^{N-1} c_n e^{-i\omega_0 n} \right|^2}{\sum_{n=0}^{N-1} |c_n|^2} \leq N. \quad (7)$$

The G_{SNR} numerator is proportional to the energy of the demodulated signal at $\omega = \omega_0$, while the denominator is proportional to the filtered noise energy. The highest $G_{\text{SNR}} = N$ is obtained only for LS-PSA in which $\omega_0 = 2\pi/N$; otherwise $G_{\text{SNR}} < N$ [11]. For example, the 7-step linear least-squares PSA (LS-PSA) has the following FTF [11],

$$H(\omega) = \sum_{n=0}^6 e^{i\omega_0 n} e^{-in\omega}; \quad (\omega_0 = 2\pi/7). \quad (8)$$

And the plot of the periodic $|H(\omega)|$ is shown in Fig. 1.

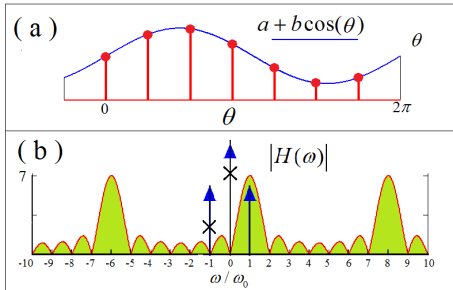


Fig. 1. Panel (a) shows 7 linear samples of a continuous fringe. Panel (b) shows the FTF of the 7-step linear LS-PSA [10]. Due to symmetry, this LS-PSA rejects many distorting harmonics at $\{-10, -9, -8, -7, -5, -4, -3, -2, 2, 3, 4, 5, 6, 7, 9, 10\}$ within the frequency range $[-10, 10]$.

Nonlinear phase-steps PSA. We describe nonuniform temporal samples from Eq. (1) as,

$$I(t_n; \varphi) = \int_{-\infty}^{\infty} [a + b \cos(\varphi + \omega_0 t)] \delta(t - t_n) dt. \quad (9)$$

Being t_n nonuniform sampling times. It is common practice to label the fringe samples by their nonlinear phase-steps as,

$$I(\theta_n; \varphi) = a + b \cos(\varphi + \theta_n); \quad (\theta_n = \omega_0 t_n). \quad (10)$$

Note that the angular frequency and sampling times are irrelevant. Therefore, from now on we will work with normalized frequency $\omega_0 = 1.0$ (radians/second). We then use θ_n instead of $(\theta_n / 1.0)$. We remark that θ_n are known. Figure 2 shows a possible realization of 9 nonuniform sampled fringe (red dots), and the Fourier spectra of the continuous-time fringe.

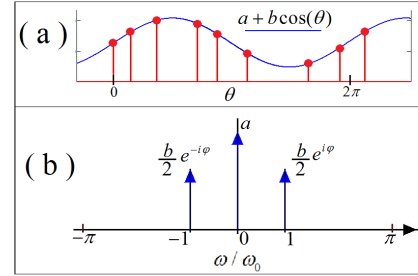


Fig. 2. Panel (a) shows 9 nonuniform phase-shifted samples of a continuous fringe at pixel (x, y) . Panel (b) shows the Fourier spectra of the continuous fringe for $\theta \in \mathbb{R}$.

FTF for nonuniform phase-stepped PSAs. Our specific goal is to find a NL-PSA as a linear combination of the nonuniform phase-stepped interferograms as,

$$Ae^{i\hat{\phi}} = \sum_{n=0}^{N-1} c_n^* I(\theta_n; \varphi); \quad (c_n \in \mathbb{C}). \quad (11)$$

Following the same receipt as linear PSAs [11], the NL-PSA's impulse response is given by,

$$h(t) = \sum_{n=0}^{N-1} c_n \delta(t - \theta_n / 1.0). \quad (12)$$

And its FTF is given by,

$$H(\omega) = F\{h(t)\} = \sum_{n=0}^{N-1} c_n e^{-i\theta_n \omega}. \quad (13)$$

If the fringe data is corrupted by AWGN, the SNR-gain (G_{SNR}) for a N -step NL-PSAs is given by,

$$G_{\text{SNR}} = \frac{\left| \sum_{n=0}^{N-1} c_n e^{-i\theta_n \omega} \right|^2}{\sum_{n=0}^{N-1} |c_n|^2} \leq N. \quad (14)$$

The equality is obtained if, and only if, $\theta_n = 2\pi n / N$; reducing to the standard linear LS-PSA (see Eq. (7)).

Three step NL-PSA. The *minimum* (normalized) quadrature conditions are,

$$H(-1) = 0; \quad H(0) = 0; \quad H(1) = 1. \quad (15)$$

According to these $H(\omega)$ constraints, one needs to solve for (c_0, c_1, c_2) , for the *known* phase-steps $(\theta_0 = 0, \theta_1, \theta_2)$ as,

$$\sum_{n=0}^2 c_n e^{i\theta_n} = 0; \quad \sum_{n=0}^2 c_n = 0; \quad \sum_{n=0}^2 c_n e^{-i\theta_n} = 1. \quad (16)$$

Which can be rewritten in matrix form as,

$$\begin{bmatrix} 1 & e^{i\theta_1} & e^{i\theta_2} \\ 1 & 1 & 1 \\ 1 & e^{-i\theta_1} & e^{-i\theta_2} \end{bmatrix} \begin{bmatrix} c_0 \\ c_1 \\ c_2 \end{bmatrix} = \begin{bmatrix} 0 \\ 0 \\ 1 \end{bmatrix}. \quad (17)$$

For $\theta_0 \neq \theta_1 \neq \theta_2$ this 3-by-3 matrix is nonsingular, and one finds $(c_0, c_1, c_2)^T$. The explicit NL-PSA formula is then,

$$Ae^{i\hat{\phi}} = c_0^* I(\theta_0; \varphi) + c_1^* I(\theta_1; \varphi) + c_2^* I(\theta_2; \varphi). \quad (18)$$

This 3-step NL-PSA is error-free ($\hat{\phi} = \varphi$) for noiseless, non-distorted, temporal fringes. Figure 3(a) shows 3 nonuniform phase samples, and the FTF which phase demodulate them.

Five phase-steps NL-PSA. With more than 3 nonuniform phase-stepped fringes, one may reject more fringe harmonics. For example if we want the FTF to have the following constraints,

$$H(-2) = 0; H(-1) = 0; H(0) = 0; H(1) = 1; H(2) = 0. \quad (19)$$

One would need 5 coefficients (c_n) as,

$$\begin{bmatrix} 1 & e^{2i\theta_1} & e^{2i\theta_2} & e^{2i\theta_3} & e^{2i\theta_4} \\ 1 & e^{i\theta_1} & e^{i\theta_2} & e^{i\theta_3} & e^{i\theta_4} \\ 1 & 1 & 1 & 1 & 1 \\ 1 & e^{-i\theta_1} & e^{-i\theta_2} & e^{-i\theta_3} & e^{-i\theta_4} \\ 1 & e^{-2i\theta_1} & e^{-2i\theta_2} & e^{-2i\theta_3} & e^{-2i\theta_4} \end{bmatrix} \begin{bmatrix} c_0 \\ c_1 \\ c_2 \\ c_3 \\ c_4 \end{bmatrix} = \begin{bmatrix} 0 \\ 0 \\ 0 \\ 1 \\ 0 \end{bmatrix}. \quad (20)$$

One may also change the desired FTF's constraints to,

$$H(-1) = 0; H(0) = 0; H(1) = 1; H(2) = 0; H(3) = 0. \quad (21)$$

Then the five coefficients (c_n) change to,

$$\begin{bmatrix} 1 & e^{i\theta_1} & e^{i\theta_2} & e^{i\theta_3} & e^{i\theta_4} \\ 1 & 1 & 1 & 1 & 1 \\ 1 & e^{-i\theta_1} & e^{-i\theta_2} & e^{-i\theta_3} & e^{-i\theta_4} \\ 1 & e^{-2i\theta_1} & e^{-2i\theta_2} & e^{-2i\theta_3} & e^{-2i\theta_4} \\ 1 & e^{-3i\theta_1} & e^{-3i\theta_2} & e^{-3i\theta_3} & e^{-3i\theta_4} \end{bmatrix} \begin{bmatrix} c_0 \\ c_1 \\ c_2 \\ c_3 \\ c_4 \end{bmatrix} = \begin{bmatrix} 0 \\ 0 \\ 1 \\ 0 \\ 0 \end{bmatrix}. \quad (22)$$

Figures 3(b) and 3(c) show 5 nonuniform samples of a phase-shifted fringe, and two different FTFs which phase-demodulate the 5 fringe-samples. The resulting 5-sample NL-PSA formula is given by,

$$Ae^{i\hat{\phi}} = \sum_{n=0}^4 c_n^* I(\theta_n; \varphi). \quad (23)$$

These two 5-step NL-PSAs are also error-free ($\hat{\phi} = \varphi$) for noiseless, non-distorted, fringes.

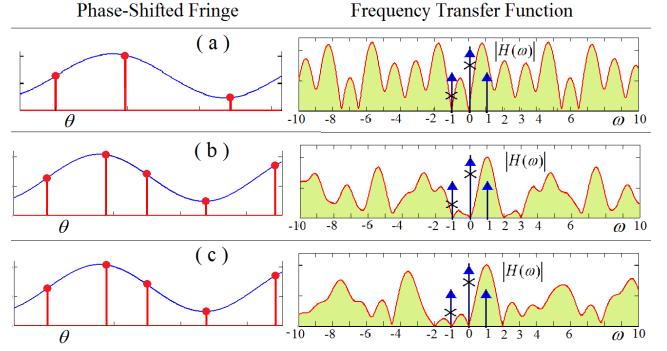


Fig. 3. As far as we know, this is the first time that FTFs for NL-PSAs are shown. Panel (a) shows 3 nonlinear phase-steps fringe data, and its corresponding FTF with zeroes at $\omega = \{-1, 0\}$. Panel (b) shows 5 nonlinear phase-steps and its FTF with zeroes at $\omega = \{-1, 0, 2, 3\}$. Panel (c) show the same data as Panel (b), but now the FTF is designed to have zeroes at $\omega = \{-2, -1, 0, 2\}$.

Harmonics rejection of the FTF-based NL-PSA. Unlike uniformly sampled linear PSA, $H(\omega)$ is not periodic for NL-PSAs. This means that the only harmonics rejected by the NL-PSA are the ones explicitly rejected in the design of its FTF. For instance consider a 7-step FTF $H(\omega)$ having the following spectral zeroes:

$$\begin{aligned} H(-2) = 0; \quad H(-1) = 0; \quad H(0) = 0; \quad H(1) = 1; \\ H(2) = 0; \quad H(3) = 0; \quad H(4) = 0. \end{aligned} \quad (24)$$

As Fig. 4 shows, this is a symmetrical distribution of spectral zeroes around $\omega = 1$. The nonlinear 7 phase-steps used are $(\theta_n) = (0, 0.78, 1.81, 3.11, 4.54, 5.93, 7.24)$. Note that the only fringe-harmonics rejected are the ones explicitly designed into its FTF.

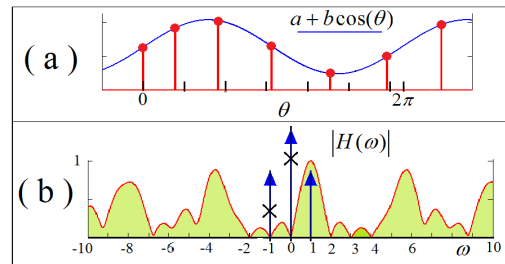


Fig. 4. Panel (a) shows seven nonlinear phase-steps of a fringe at pixel (x, y) . The phase-shifting coordinate is θ (radians). Panel (b) shows the FTF of the NL-PSA which demodulate, *error-free*, the 7 temporal samples. Note that this FTF have zeroes at $\omega = \{-2, -1, 0, +2, +3, +4\}$.

Both Fig. 1 and Fig. 4 correspond to 7-step PSAs. In Fig. 1 the LS-PSA's FTF has zeroes at: $\{-10, -9, -8, -7, -5, -4, -3, -2, -1, 0, 2, 3, 4, 5, 6, 7, 9, 10\}$. In contrast our NL-PSA has only the designed FTF's zeroes at $\{-2, -1, 0, 2, 3, 4\}$ in the same range. In other words the use of nonuniform phase-steps reduces the harmonic rejection capacity of the NL-PSA. Nevertheless, this is much better than G-PSA, AIA, and PCA-PSA which only reject the quadrature components of the fundamental fringe frequency [1-10]. This is a serious disadvantage for amplitude-distorted fringe-data because all distorting harmonics survive. Even

worst the AIA and the PCA-PSA must pre-filter its background signal at $\omega=0$ [5,9,10].

Computer simulation. We simulated 7 fringe patterns with the aforementioned phase-steps $(\theta_n)=(0, 0.78, 1.81, 3.11, 4.54, 5.93, 7.24)$ and designing the FTF to have the zeroes in Eq. (24). The resulting FTF's complex coefficients are $(c_n)=\{-0.06, 0.21-0.21i, -0.05-0.2i, -0.22, -0.04-0.22i, 0.23+0.08i, -0.07-0.1i\}$. The resulting NL-PSA is then,

$$Ae^{i\hat{\phi}} = \sum_{n=0}^6 c_n^* I(\theta_n; \varphi). \quad (24)$$

The first sample has the lowest weight $|c_0|=0.06$, meaning that its information is taken less into account. Two out of seven noiseless fringes, and its demodulated phase are shown in Fig. 5.

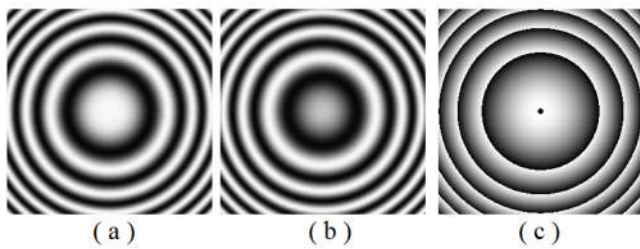


Fig. 5. Panels (a)-(b) show 2 out of 7 noiseless, nonlinear phase-stepped fringes. Panel (c) shows the *error-free* estimated phase.

We remark that the estimated phase for our FTF based NL-PSAs, is mathematically *error-free* ($\hat{\phi} = \varphi$), whenever the phase-steps (θ_n) among the interferograms are known accurately. However, error-free phase estimation is not mathematically guaranteed in PCA-PSA [10]. In the case of AIA and noiseless fringes, it normally takes many iterations to reach an error-free phase estimation [10]. In other words, for noiseless fringes, the estimated phase recovered by our NL-PSAs is as good as the one obtained by standard linear PSAs [11]. Of course, for fringes corrupted by AWGN and harmonics, we obtain a distorted demodulated phase, as it is the case for standard linear PSAs [11].

SNR gain for our specific NL-PSA. For our specific case with $(\theta_n)=(0, 0.78, 1.81, 3.11, 4.54, 5.93, 7.24)$, the SNR-gain is given by,

$$G_{\text{SNR}} = \frac{\left| \sum_{n=0}^6 c_n e^{-i\theta_n} \right|^2}{\sum_{n=0}^6 |c_n|^2} = 5.142. \quad (25)$$

Resulting in a 27% SNR-gain reduction with respect to a 7 samples linear LS-PSA ($G_{\text{SNR}}=7$).

Comparison against PCA-PSA. Before concluding we show a comparison of our FTF based NL-PSA and the PCA-PSA. It is well known that the PCA-PSA does not give, in general, an error-free phase estimation, even for noiseless nonlinear phase-stepped fringes [9,10]; this can be seen in Fig. 6. However the approximate PCA-PSA's solution may be used as initial condition for the AIA. Then the AIA, after several iterations, converges to an almost error-free phase estimation, for noiseless fringes [10].

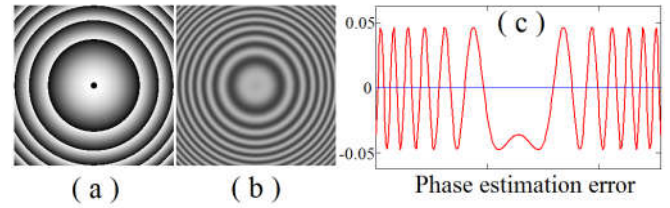


Fig. 6. Panel (a) shows the PCA-PSA's estimated phase from the noiseless fringe-data in Fig. 5. Panel (b) shows the phase estimation error. Panel (c) shows a central cut of the phase estimation error in radians. The phase error of our NL-PSA is about 10^{-15} (a numerical zero).

Conclusions. The herein proposed NL-PSA theory is a key contribution to nonlinear phase-steps interferometry in the sense that:

1) As far as we know, the spectral response (the FTF) for NL-PSAs was obtained for the first time. This FTF is in turn used to find the corresponding N -step NL-PSA formula.

2) For a given number of nonlinear phase-steps (θ_n) , our NL-PSA has the highest fringe harmonics rejection. In contrast, the G-PSA, AIA or PCA-PSA do not reject, by design, higher order harmonics of the fringe data [1-10].

3) Our FTF-based NL-PSA give us as a bonus, the signal-to-noise ratio gain (G_{SNR}) for fringes corrupted by AWGN. This contrast with G-PSA, AIA, and PCA-PSA which *do not give* a SNR estimate [1-10] from basic stochastic process theory [11,12].

4) Finally, our FTF-based NL-PSA design recovers the demodulated phase *error-free* for noiseless, non-distorted fringes. This not being the case for PCA-PSA [9,10].

References

1. J. E. Greivenkamp, Opt. Eng. **23**, 350 (1984).
2. K. Okada, A. Sato, and J. Tsujiuchi, Opt. Comm. **34**, 118 (1991).
3. I. Kong and S. Kim, Opt. Eng. **34**, 183 (1995).
4. S. Tang, in Proc. SPIE, Laser Interferometry VIII, **2860**, 34 (1996).
5. Z. Wang and B. Han, Opt. Lett. **29** 1671 (2004).
6. K. Hibino, B. F. Oreb, D. I. Farrant, and K. G. Larkin, J. Opt. Soc. Am. A **4**, 918 (1997).
7. R. Langoju, A. Patil, and P. Rastogi, Opt. Lett. **31**, 1058 (2006).
8. G. A. Ayubi, C. D. Perciante, J. L. Flores, J. M. Di Martino, and J. A. Ferrari, Appl. Opt., **53**, 7168 (2014).
9. J. Vargas, J. A. Quiroga, and T. Belenguer, Opt. Lett. **36**, 1328 (2011).
10. J. Vargas, C. O. S. Sorzano, J. C. Estrada, and J. M. Carazo, Opt. Comm. **286**, 130 (2013).
11. M. Servin, J. A. Quiroga, and M. Padilla. Fringe Pattern Analysis for Optical Metrology. Wiley-VCH (2014).
12. A. Papoulis, Probability, Random Variables, and Stochastic Processes, McGraw-Hill (1991).

Full References

1. J. E. Greivenkamp, "Generalized data reduction for heterodyne interferometry," *Opt. Eng.* **23**(4), 350-352 (1984).
2. K. Okada, A. Sato, and J. Tsujiuchi, " Simultaneous calculation of phase distribution and scanning phase shift in phase shifting interferometer," *Opt. Comm.* **34**(3), 118-124 (1991).
3. I. Kong and S. Kim, "General algorithm of phase-shifting interferometry by iterative least-squares fitting," *Opt. Eng.* **34**(1), 183-188 (1995).
4. S. Tang, "Generalized algorithm for phase shifting interferometry," *Proc. SPIE, Laser Interferometry VIII: Techniques and Analysis*, **2860**, 34-44 (1996).
5. Z. Wang and B. Han, "Advanced iterative algorithm for phase extraction of randomly phase-shifted interferograms," *Opt. Lett.* **29**(14), 1671-1673 (2004).
6. K. Hibino, B. F. Oreb, D. I. Farrant, and K. G. Larkin, *J. Opt. Soc. Am. A* **4**, 918, (1997)
7. R. Langoju, A. Patil, and P. Rastogi, "Phase-shifting interferometry in the presence of nonlinear phase steps, harmonics, and noise," *Opt. Lett.* **31**(8), 1058-1060 (2006).
8. G. A. Ayubi, C. D. Perciante, J. L. Flores, J. M. Di Martino, and J. A. Ferrari, "Generation of phase-shifting algorithms with N arbitrarily spaced phase-steps," *Appl. Opt.*, **53**(30), 7168-7176 (2014).
9. J. Vargas, J. A. Quiroga, and T. Belenguer, "Phase-shifting interferometry based on principal component analysis," *Opt. Lett.* **36**(8), 1326-1328 (2011).
10. J. Vargas, C. O. S. Sorzano, J. C. Estrada, and J. M. Carazo, "Generalization of the Principal Component Analysis algorithm for interferometry," *Opt. Comm.*, **286**, 130-134 (2013).
11. M. Servin, J. A. Quiroga, and M. Padilla. *Fringe Pattern Analysis for Optical Metrology, Theory, Algorithms, and Applications*. Wiley-VCH (Weinheim, Germany 2014).
12. A. Papoulis, *Probability, Random Variables, and Stochastic Processes*, McGraw-Hill (Singapore 1991).